15CV-0323/2015-01-2749

Pneumatically Balanced Heavy Truck Air Suspensions for Improved Roll Stability

Yang Chen, Mehdi Ahmadian, Andrew Peterson
Virginia Tech

Abstract

This study provides a simulation evaluation of the effect of maintaining balanced airflow, both statically and dynamically, in heavy truck air suspensions on vehicle roll stability. The model includes a multi-domain evaluation of the truck multi-body dynamics combined with detailed pneumatic dynamics of drive-axle air suspensions. The analysis is performed based on a detailed model of the suspension's pneumatics, from the main reservoir to the airsprings, of a new generation of air suspensions with two leveling valves and air hoses and fittings that are intended to increase the dynamic bandwidth of the pneumatic suspensions. The suspension pneumatics are designed such that they are able to better respond to body motion in real time. Specifically, this study aims to better understand the airflow dynamics and how they couple with the vehicle dynamics. The pneumatic model is coupled with a roll-plane model of the truck to evaluate the effect of the suspension pneumatic dynamics on the body roll, as well as the force transmission to the sprung mass. The results of the study show that maintaining a balanced airflow through the suspension improves the dynamic responsiveness of the suspension to steering, causing less body roll.

Keywords: Air suspensions, balanced airflow, pneumatic model, heavy truck.

1. Introduction

The airspring suspension is considered to be the "standard" suspension in nearly all highway trucks and majority of on- and off-highway vehicles. From 1996 to 2013, the applications of air suspension on heavy trucks have increased from 36% to 75% of the truck industry in North America, mainly because of their load leveling capability and improved ride. Generally, an air suspension system has three basic components: air supply elements, airsprings and leveling valve(s). Airsprings work by generating a restoring force in response to compression of air in an elastic bag with metal caps at each end [1]. The leveling valve can maintain the specified height of the suspension by adjusting the air pressure of the airsprings [2]. There exist various types of air suspensions on trucks, depending on the dynamic need of the vehicle and its intended use.

A few studies in the past have developed mathematical models for pneumatic suspensions in order to better understand their dynamic behavior. Nieto and Morales obtained a nonlinear model of a pneumatic suspension based on an experimental characterization [3], and proposed an adaptive pneumatic suspension system by selecting the most appropriate plumbing configuration between airspring and auxiliary tank [4]. Xu [5] and Bao [6] built a detailed pneumatic system model coupled with a vehicle dynamic model in Simulink. Kim [7] and Moshchuk [8] developed a pneumatic suspension model implemented in AMEsim, without including change in the effective area of the airspring.

This study extends the past models on pneumatic suspensions by developing a model that couples the pneumatic dynamics with multibody dynamics of the truck. AMEsim is used to model the pneumatic suspensions system, from the air supply (tank) to the

airsprings. The model includes the effect of all of the components used in the airsprings. Additionally, the dynamics of the truck are included in AMEsim through a 9 degree of freedom model that includes the heave, pitch, and roll of the body, as well as the unsprung mass dynamics of the front and dual rear axles. The model is applied to study how changing the pneumatic configuration of the air suspension affects the truck dynamics. Specifically, the results presented here include a common air suspension arrangement with one leveling valve, and another design that includes two leveling valves and a side to side symmetric plumbing arrangement. The results show that the latter (referred to as a "balanced" arrangement) provides better body roll control, as compared to the former (referred to as an "OE" arrangement).

2. Model Description

The original equipment (OE) plumbing arrangement of twin-axle air suspensions is shown in Figure 1 (right). One leveling valve is applied to control four airsprings, and the four airsprings are connected in series by the pipes. The other plumbing arrangement on rear tandem axles is illustrated in Figure 1 (left). Two leveling valves are used to control two airsprings on each side. Air pipes are of equal length from the air tank to the leveling valve, and from the leveling valve to the airsprings. Consequently, a perfect symmetric attribute about the truck centerline and rear tandem axle's centerline is possessed by the "balanced" plumbing arrangement. In addition, the pipe is designed with a larger diameter in the balanced suspension than in the OE suspension.

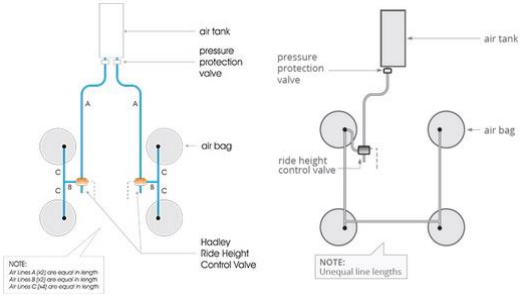

Figure 1. Balanced (left) and Original Equipment (OE) (right) configurations on rear tandem axle [9]

2.1 Pneumatic Model

2.1.1 Airspring Model

According to the Ideal Gas Law, the relation between pressure p_s, temperature T_s, mass m_s, and volume V_s in an airspring can be expressed as [10, 11, 12]:

$$p_s V_s = \frac{m_s}{M_s} R T_s \tag{1}$$

In the isentropic process, two equations can be written as:

$$p_s \left(\frac{V_s}{m_s}\right)^n = p_{s0} \left(\frac{V_{s0}}{m_{s0}}\right)^n \tag{2}$$

$$\frac{T_s}{T_{s0}} = \left(\frac{p_s}{p_{s0}}\right)^{\frac{n-1}{n}} \tag{3}$$

The mass change in airspring depends on mass flow supplying to the airspring from the air tank or exhausting to the atmosphere through the leveling valve, airflow between coupling airsprings, and leakage in the airspring. The volume change in airspring is caused by two factors: the change of airspring height and the elastic radial deformation. Then using the equations above to yield the first order differential equation of pressure in the airspring:

$$\dot{p}_s = -\frac{n R T_{s0}}{V_s} \left(\frac{p_s}{p_{s0}}\right)^{\frac{n-1}{n}} \dot{m}_s - \frac{n p_s}{V_s} \dot{V}_s \tag{4}$$

where $\dot{m}_s = \dot{m}_l + \dot{m}_c + \dot{m}_k$. It is positive for inflating and negative for deflating. $\dot{m}_l$ and $\dot{m}_c$ are mass flow through the leveling valve and between the coupled airsprings, respectively. Here, leakage $\dot{m}_k$ is considered to be zero. In addition, the change in volume is expressed as :

$$\dot{V}_s = \frac{\partial V_s}{\partial h} \dot{h} + \frac{\partial V_s}{\partial A} \dot{A} \tag{5}$$

It is considered that the tractor is equipped with the rolling lobe airsprings with the positive tapered piston. Here, it is assumed that the effective area changes according to a linear equation [3], A =

$A_0(1-kx)$. A_0 is initial piston area, and x is suspension deflection. The coefficient k=0.02 means that the change in effective area is $0.02A_0$ with one inch deflection. One additional equation is incorporated to calculate pressure force:

$$F = (p_s - p_a)A \quad (6)$$

Next, based on the equations, the airspring is modeled on the AMEsim platform [13] as displayed in Figure 2. One pneumatic chamber with moving body is employed to reflect the change of volume due to the vertical displacement of the airspring. In order to ensure the change in volume due to the change in effective area to be included according to equation (5), an additional normal pneumatic chamber is used. Those pneumatic chambers can produce the pressure forces according to equation (6), which are separately transmitted to sprung mass and unsprung mass.

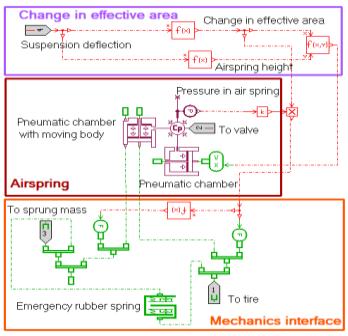

Figure 2. Model of airspring

2.1.2. Leveling Valve Model

The leveling valve can be functionally considered as an equivalent orifice. The mass flow rate through the leveling valve is affected by upstream pressure and downstream pressure and the effective area of the orifice. The amount of the valve effective flow area is related to the displacement of the lever caused by the vertical displacement of the driving axle with respect to the truck body. The mass flow rate equation can be expressed as [5]:

$$\dot{m}_l = \left(\frac{2}{n+1}\right)^{\frac{n+1}{2(n-1)}}\sqrt{\frac{n}{RT_l}}p_u S \quad \left(\frac{p_d}{p_u} \le b\right) \quad (7)$$

$$\dot{m}_l = \left(\frac{2}{n+1}\right)^{\frac{n+1}{2(n-1)}}\sqrt{\frac{n}{RT_l}}p_u S\sqrt{1-\left(\frac{\frac{p_d}{p_u}-b}{1-b}\right)}$$

$$\left(b < \frac{p_d}{p_u} \le 1\right) \quad (8)$$

In the simulation, the leveling valve model is developed based on the three position, three port proportional pneumatic valve in AMEsim as illustrated in Figure 3. In this valve model, the spool moves according to a second order transfer function. The natural frequency is considered to be so large that the response time of the valve can be negligible. According to the plumbing configuration, the displacement of the airspring on the front driving axle (middle axle) is sensed by the lever as the input signal of controlling the valve opening. In order to achieve the response with dead band, an extra controller for the leveling valve is built as displayed in Figure 3. In addition, the deflating port T of the leveling valve is modeled as an ideal pressure source, which is atmosphere pressure.

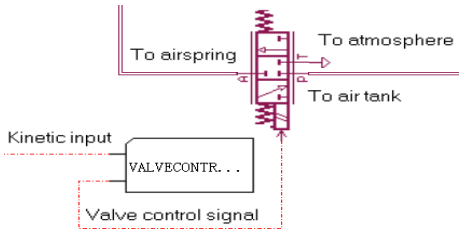

Figure 3. Leveling valve model

2.1.3. Pipe and Tank Models

The pressure loss and the compressibility of the gas are taken into account in the pipe model, where the outlet flow is attenuated and delayed by the time, $\frac{L_t}{c}$. The flow equation at the outlet of the tube is [14]:

$$\text{If } t < \frac{L_t}{c}, \dot{m}_{outlet}(L_t, t) = 0 \quad (9)$$

$$\text{If } t > \frac{L_t}{c}, \dot{m}_{outlet}(L_t, t) = e^{-\frac{R_t R T L_t}{2Pc}}\dot{m}_{inlet}(t) \quad (10)$$

The tube resistance, R_t, which can be obtained from

the equation of pressure drop along the tube, is expressed as:

$$\Delta p = f\frac{L_t}{D}\frac{\rho u^2}{2} = R_t u L_t \quad (11)$$

The tube resistance becomes $R_t = 32\mu/D^2$ for fully developed laminar flow. For wholly turbulent flow, $R_t = 0.158\mu/D^2 R_e^{\frac{3}{4}}$. In the simulation, the air tank is simply modeled as an ideal source, and the standard check valve model in the AMEsim pneumatic library is applied to represent the check valve in the pneumatic circuit. Some main parameters used in the pneumatic system simulation may be found in Table 1 in Appendix A.

2.2 Truck Multibody Dynamic Model

The tri-axle tractor dynamic model schematic is shown in Figure 4. The degrees of freedom of the model are: bounce z, pitch θ, and roll φ of sprung mass, bounce of six unsprung masses. In this mode, tire damping is ignored.

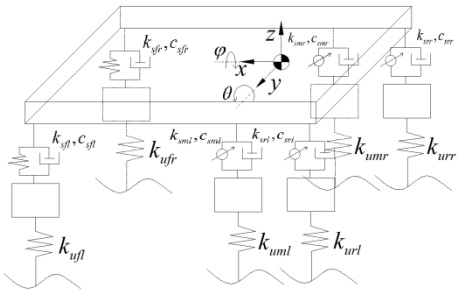

Figure 4. Truck multibody dynamic model schematics

Three equations of motion are used to model the sprung mass with three DOFs. The sprung mass vertical motion equation is:

$$m\ddot{z} = F_{Kfl} + F_{cfl} + F_{Kfr} + F_{Cfr} + (F_{Kml} - F_0) + F_{Cml} + (F_{Kmr} - F_0) + F_{Cmr} + (F_{Krl} - F_0) + F_{Crl} + (F_{Krr} - F_0) + F_{Crr} \quad (12)$$

The sprung mass motion equation for pitch is

$$I_p\ddot{\theta} = b_1[(F_{Kml} - F_0) + F_{Cml} + (F_{Kmr} - F_0) + F_{Cmr}] + b_2[(F_{Krl} - F_0) + F_{Crl} + (F_{Krr} - F_0) + F_{Crr}] - a(F_{Kfl} + F_{Cfl} + F_{Kfr} + F_{Cfr}) + mgr_\theta\theta \quad (13)$$

The sprung mass motion equation for roll is:

$$I_r\ddot{\varphi} = \frac{d}{2}[(F_{Kml} - F_0) + F_{Cml} + (F_{Krl} - F_0) + F_{Crl}] - \frac{d}{2}[(F_{Kmr} - F_0) + F_{Cmr} + (F_{Krr} - F_0) + F_{Crr} + mg\varphi r_\varphi + \frac{c}{2}(F_{Kfl} + F_{Cfl}) - \frac{c}{2}(F_{Kfr} + F_{Cfr}) - ma_{lateral}r_\varphi \quad (14)$$

The bounce of attachment points on the vehicle body of six suspensions are:

$$z_{fl} = z - a\theta + \frac{c}{2}\varphi \qquad z_{mr} = z + b_1\theta - \frac{d}{2}\varphi$$

$$z_{fr} = z - a\theta - \frac{c}{2}\varphi \qquad z_{rl} = z + b_2\theta + \frac{d}{2}\varphi$$

$$z_{ml} = z + b_1\theta + \frac{d}{2}\varphi \qquad z_{rr} = z + b_2\theta - \frac{d}{2}\varphi$$

On the basis of the equations above, a sprung mass dynamic model is established using the Signal and Control Library in AMEsim. The suspension is modeled according to a quarter car model in the Mechanical Library and integrated with the pneumatic model represented in the previous section based on the relationship expressed in Figure 20 in Appendix C. Corresponding parameters used in simulating the multi-body truck model can be obtained in Table 2 of Appendix B.

3. Model Function Validation

3.1. Validation for Airspring Model

A simulated "testing bench" is built, as depicted in Figure 5, for functionally verifying the airspring model. In the "testing," the bottom of the airspring is fixed. Initial pressure in the airspring is set to be 70 psi, and initial height is kept at 10 inches. Curves of deflection-volume, deflection-pressure, and deflection-force are obtained and illustrated in Figure 6. Those nonlinear curves are in line with the

expectation of the dynamic characteristic of an airspring, indicating that the airspring model can be used for further building the whole system model for the simulation study.

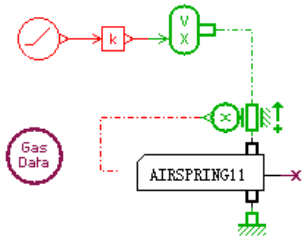

Figure 5. Model used for validation of airspring model

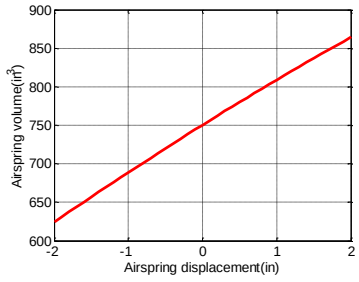

(a)

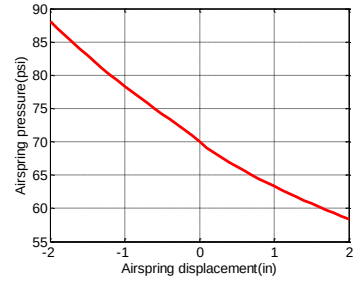

(b)

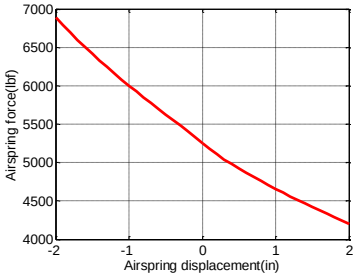

(c)

Figure 6. Effects of suspension deflection on airspring volume (a), airspring pressure (b) and airspring force (c)

3.2. Validation for Leveling Valve

In order to functionally verify the leveling valve model, a "testing bench" model is also established as represented in Figure 7. Pressures of port P and port T are set to be atmosphere pressure. Three different pressures, 29 psi, 44 psi, and 58 psi, are simulated at port A in sequence. The effects of leveling valve control arm position on mass flow rate at supply and purge ports are demonstrated in Figure 8a, where we can see that the flow characteristics are nonlinear and nonsymmetrical for inflating and deflating even with same pressure difference. Specifically, there is a dead zone around the origin that is regarded as the neutral position of the valve where air will not flow through the valve. Furthermore, it is observed in Figure 8a that the mass flow rate for either air exhaust or air supply raised with pressure at port A is increased. The flow rate also relies on the amount of flow area that is associated with the displacement of the control arm as depicted in Figure 8b. Results of the simulation clearly show an agreement with the mass flow rate equations (7) and (8) of the leveling valve. Until now, the airspring model and the leveling valve model have been validated as achieving their functions as expected and they can be applied in the simulation of the pneumatic suspension subsystem.

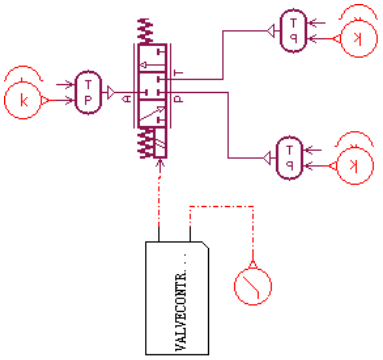

Figure 7. Model used for validation of leveling valve model

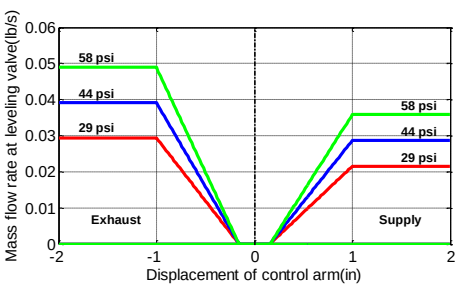

(a)

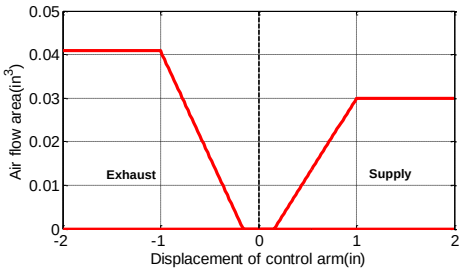

(b)

Figure 8. Effects of control arm displacement on mass flow rate (a) and flow area (b) through the leveling valve

3.3. Balanced Pneumatic Suspension Validation

A half-balanced pneumatic suspension model on driving axles is built such that a bump is encountered separately by the middle and rear wheels with the vehicle body grounded, as depicted in Figure 9. The height of the bump is assumed to be 3 inches. The time for each wheel across the bump is 0.06s, and the time delay between the two axles for encountering the bump is 0.32s. The results are shown in Figures 10, 11, and 12, and the leveling valve can be activated immediately for inflating when the deflection of air suspension on the middle driving axle is over the dead band. As we can also see in Figures 10a and 11, in the short period after bumping the mid axle at 0.5 second, the pressure in the mid airspring increases while the mid airspring is compressed. At that moment, the pressure difference between the two interconnected airsprings and inflation through the leveling valve allow air flow into the rear airspring, leading to a small increase in the displacement of the rear airspring with the rear wheel compressed as shown in Figure 10b. According to the equation (4), due to the air inflows from the mid airspring and leveling valve, pressure in the rear airspring increases after 0.5 seconds as depicted in Figure 11. Additionally, as soon as the excitation force disappears, the front-rear interconnected airsprings can quickly balance the pressure.

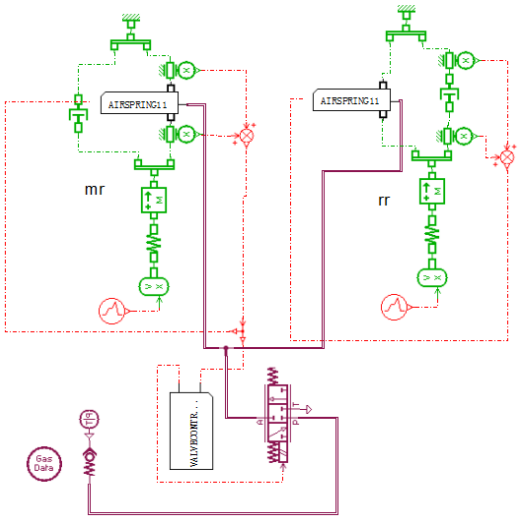

Figure 9. Model used for verifying a pair of balanced air suspensions

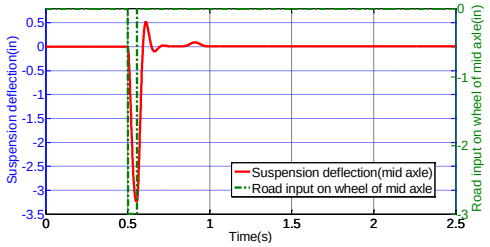

(a)

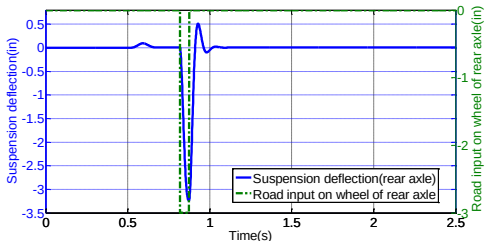

(b)

Figure 10. Time trace of suspension deflection on middle axle (a) and rear axle (b) with a 3 inch bump input

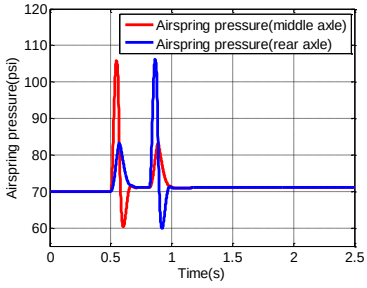

Figure 11. Time trace of airspring pressure

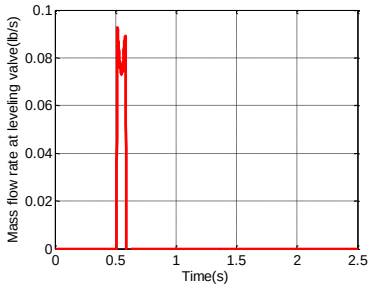

Figure 12. Time trace of mass flow rate at leveling valve

Following the functional validation of the component models and the pneumatic suspension subsystem model, the aligned complete system model shown in Figure 21 of Appendix C can be used to study and compare the effects of the two air suspensions on the truck roll performance. The “test bench” models built above could also assist in design of the pneumatic experiment in the future.

4. Simulation Results

To assess the performance of the air suspensions on roll stability, two different steering maneuvers, cornering and S-turn, are simulated. For cornering simulation, it is assumed that a loaded truck enters a right turn for 5 seconds, and a lateral acceleration is applied on the center of gravity (CG) of the loaded tractor in the left direction, which is depicted in Figure 13. Here, we take $V^2/R = 0.15g$, with V being the cornering speed of the vehicle and R being the curve radius. When the path is an 'S' curve, the lateral acceleration is approximated as a sinusoidal wave input with a magnitude of 0.15g and a frequency of 0.16 Hz as depicted in Figure 14. In the simulation, the road is assumed to be perfectly smooth.

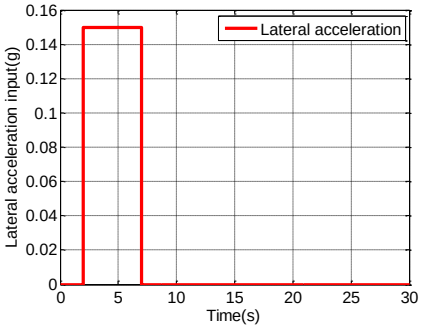

Figure 13. Lateral acceleration for a right-hand turn

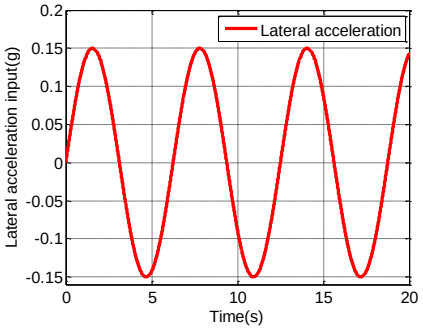

Figure 14. Lateral acceleration input for S-turn

The change in pressure of airsprings on the driving axles obtained by the simulation is represented in Figures 15a, 15b, 16a, and 16b. As can be seen by comparing with OE airsprings in Figures 15a and 15b, during cornering, higher pressure can be obtained in balanced airsprings on the outer side, while simultaneously, there is lower pressure in balanced airsprings on the inner side. The results indicate a larger difference of air pressure from side to side in balanced airsprings than OE airsprings among driving axles. It is found from the simulation results of S-turns in Figures 16a and 16b that the balanced airspring is able to remain higher and lower pressure than OE airspring respectively in compression and extension, except the OE airspring on the left side of middle driving axle, which's displacement is sensed by the lever of the leveling valve in OE pneumatic system and tends to have same pressure change as balanced air suspension. The design of equal length pipes from the leveling valves to the airsprings in a balanced pneumatic arrangement allows two airsprings on either side to equally share air mass flow through the leveling valve. Consequently, the balanced airsprings are

able to maintain improved equal pressure front and rear that doesn't happen in OE airsprings while the truck body is rolling, as shown in Figures 15a, 15b, 16a, and 16b.

It is observed in Figures 15c, 15d, 16c, and 16d that a larger restoring force is produced by the balanced airspring than the OE airspring to keep the suspension in balance. By comparing airspring forces on the right and left sides, it is found that the side-to-side force difference in balanced airsprings is larger than in OE airsprings to better resist the overturning moment of truck body roll. Furthermore, as we can see in Figures 15c, 15d, 16c, and 16d, balanced air suspensions on either side of the driving axles can provide equal suspension force to sprung mass. For OE suspensions, uneven airspring forces are transmitted to the sprung mass and the driving axle during cornering and S-turns. As illustrated in Figures 15c and 16c, there is a relatively large airspring force on the left side OE airspring of the middle axle, which implies a significant increase in tire wear.

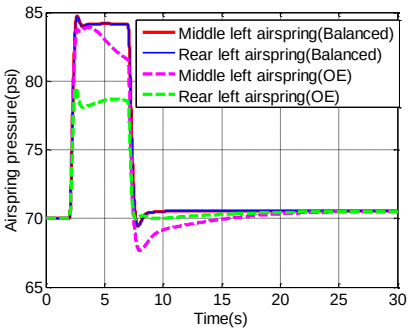

(a) Airspring pressure on left side (cornering)

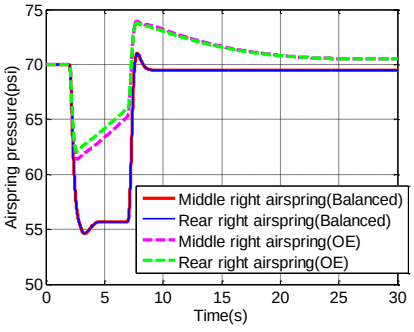

(b) Airspring pressure on right side (cornering)

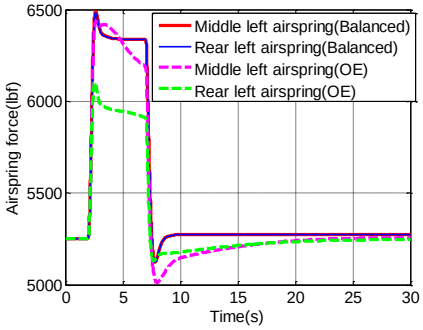

(c) Airspring force on left side (cornering)

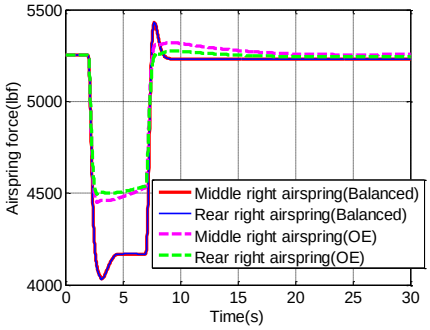

(d) Airspring force on right side (cornering)

Figure 15. Time trace of airspring pressure on tandem driving axles and airspring force transmitted to sprung mass for a right-hand cornering

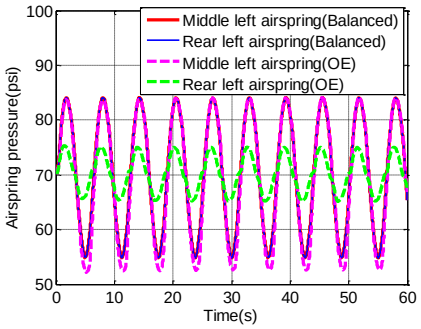

(a) Airspring pressure on left side (S-turn)

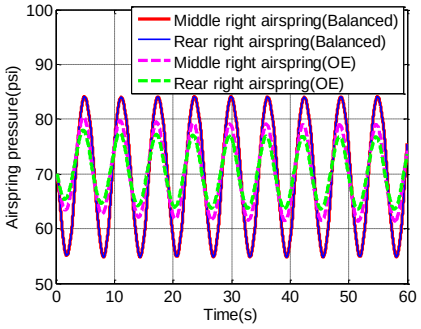

(b) Airspring pressure on right side (S-turn)

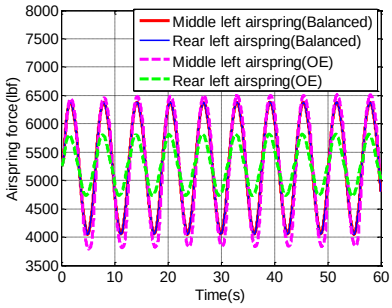

(c) Airspring force on left side (S-turn)

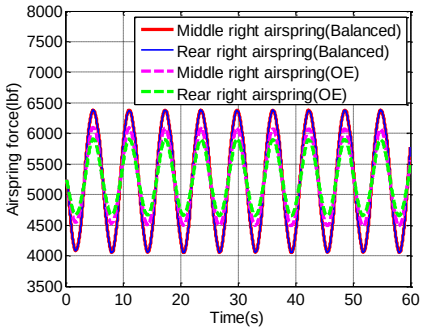

(d) Airspring force on right side (S-turn)

Figure 16. Time trace of airspring pressure on tandem driving axles and airspring force transmitted to sprung mass for S-turn

Suspension deflection on the driving axles and the mass flow rate at the leveling valves are shown respectively in Figures 17a-d, and Figures 18a-b. Figures17a-d indicate that, in comparison with the OE suspension, the balanced suspension has small deflection and faster dynamic response to the load input. This implies that the balanced suspension has a higher bandwidth. Comparing the suspension deflection and flow rate at the leveling valve, Figures 18a and 18b indicate that the leveling valves on the opposite sides have opposition actions, with one adding air to the airsprings (on the jounce side) while the other one purges air (the rebound side), in response to the body roll. This dynamic results in better return of the body to a leveled position after it has been subjected to lateral forces (acceleration). The larger air hose diameters in the balanced pneumatic suspension results in less air flow resistance into or out of each airspring as described in equation (10), which provides the dynamic of adjusting air pressure in the airspring. Moreover, the lack of plumbing connection between the right and left airsprings plays an important role in maintaining the side-to-side balance forces. The leveling valve in the OE suspension provides unwanted adjustment of airspring pressure on the sides opposite the leveling valve, although the small diameter of the pipes reduces the transient air pressure. As observed in Figures 17a-d, uneven and slow dynamic responsiveness of the OE air suspensions among the rear driving axles is obtained.

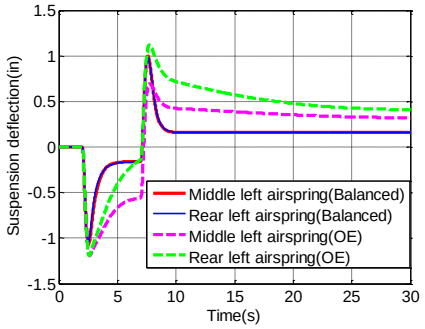

(a) Suspension deflection on left side (cornering)

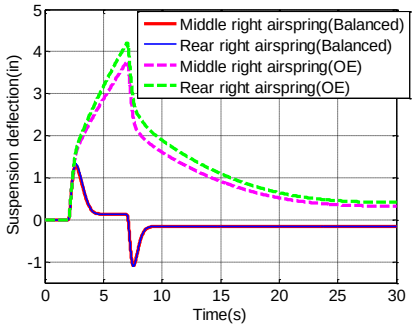

(b) Suspension deflection on right side (cornering)

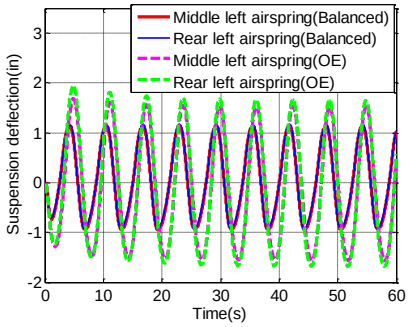

(c) Suspension deflection on left side (S-turn)

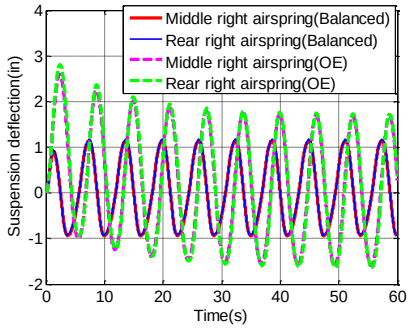

(d) Suspension deflection on right side (S-turn)

Figure 17. Time trace of suspension deflection on rear tandem axles for a right-hand cornering and S-turn

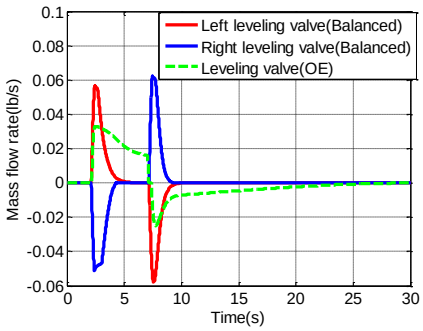

(a) Flow rate at leveling valve (cornering)

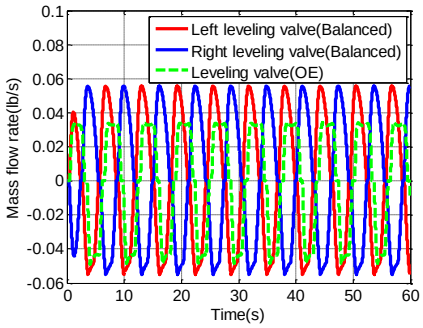

(b) Flow rate at leveling valve (S-turn)

Figure 18. Time trace of flow rate at leveling valves for cornering and S-turn

Figure 19a illustrates that when the lateral force is applied, the roll angle quickly reduces by the balanced suspension to a small value, balancing and keeping the truck body level. Additionally, the truck equipped with the balanced air suspension experiences a smaller maximum roll angle. When the lateral forces disappear after 7 seconds as shown in Figure 19a, the balanced suspension enables the truck body to quickly return to the unrolled orientation with a shorter settling time than the OE suspension. As shown in Figure 19c, in S-turn, the balanced suspension results in a smaller roll angle as compared with the OE suspension. To the extent that the roll and pitch dynamic of the truck body couple, the balanced suspension results in less body pitch during the lateral maneuvers, as shown in Figures 19b and 19d.

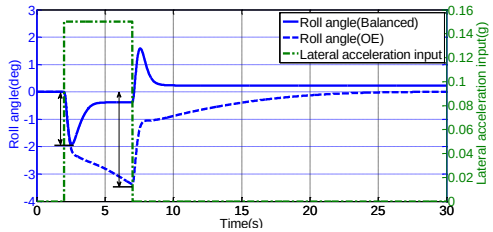

(a) Roll angle (cornering)

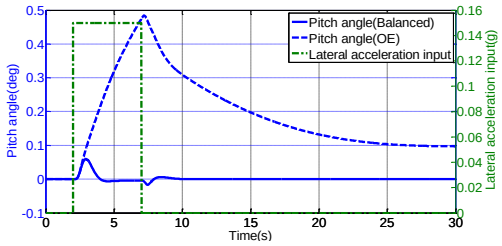

(b) Pitch angle (cornering)

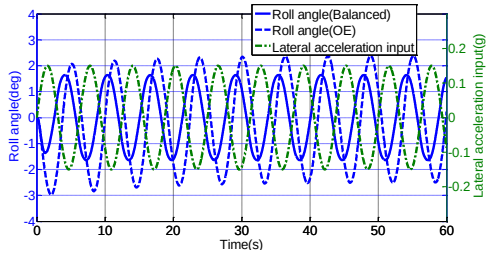

(c) Roll angle (S-turn)

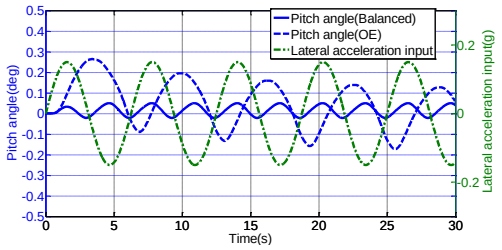

(d) Pitch angle (S-turn)

Figure 19. Time trace of roll angle and pitch angle for cornering and S-turn

5. Conclusions

In this paper, the air suspension model coupled with truck multibody dynamics has been developed and presented in detail. Based on functionally validated pneumatic components and suspension subsystem models, the complete system model is employed to compare and analyze performance of two air suspensions with different plumbing arrangements on roll stability. The results of the simulation are summarized as follows:

(1) During truck body roll, higher and lower pressure in the balanced airsprings are obtained, respectively, on jounce and rebound than for the OE airsprings, except for the airspring on the left side of the middle axle.

(2) In cornering and S-turns, the balanced airsprings on the rear driving axles are able to maintain a larger difference in pressure from side to side than the OE airsprings and can produce equal pressure front and rear.

(3) In cornering and S-turns, compared with the OE air suspension, the balanced air suspension produced a larger restoring force to keep the suspension in balance.

(4) In cornering and S-turns, less suspension travel and quicker dynamic response are obtained for the balanced suspension compared with the OE suspension.

(5) During cornering and S-turns, lower roll and pitch angles are experienced by the truck with the balanced air suspensions, improving roll stability.

References

1. Fox, M.N., Roebuck, R.L., Cebon, D., "Modeling rolling lobe air springs," International Journal of Heavy Vehicle Systems, Vol.14, No. 3, 2007, pp. 254-270.

2. Nahajima, T., Shimodawa, Y., Mizuno, M., Sugiyama, H., "Air Suspension System Model Coupled With Leveling and Differential Pressure Valves for Railroad Vehicle Dynamics Simulation," Journal of Computational and Nonlinear Dynamics, Vol. 9, July, 2014, pp. 031006, 1-9, doi:10.1115/1.4026275.

3. Nieto, A.J., Morales, A.L., Gonzalez, A., Chicharro, J.M., Pintado, P., "An Analytical Model of Pneumatic Suspensions Based on An Experimental Characterization," Journal of Sound and Vibration, Vol. 313, 2008, pp. 290-307, doi: 10.1016/j.jsv.2007.11.027.

4. Nieto, A.J., Morales, A.L., Chicharro, J.M., Pintado, P., "An Adaptive Pneumatic Suspension System for Improving Ride Comfort and Handling," Journal of Vibration and Control, June, 2014, pp. 1-12, doi: 10.1177/1077546314539717.

5. Xu, X., Chen, Z.Z., Huang, J.J., Li, Z.X., "Dynamic Modeling and Characteristic Simulation of Charging-discharging System for Electronically Controlled Air Suspension," Journal of System Simulation, Vol. 23, No. 6, June, 2011, pp.1225-1228.

6. Bao, W.N., Chen, L.P., Zhang, Y.Q., Zhang, G.S., "A Study on Dynamics Model for Coupled Air Springs Suspension System," Automotive Engineering, Vol.30, No.3, 2008, pp. 231-234.

7. Kim, H., Lee, H., "Height and Leveling Control of Automotive Air Suspension System Using Sliding Mode Approach," IEEE Transactions on Vehicular Technology, Vol. 60, No. 5, June, 2011, pp. 2027-2041.

8. Moshchuk, N., Li, Y.J., Opiteck, S., "Air Suspension System Model and Optimization," SAE International, 2011, doi: 10.4271/2011-01-0067.

9. Richardson, S., Sandvik, A., Jones, C., Josevski N., Pei W., “The Comparative Testing of Single and Double Ride Height Control Valve Suspension Control System,” 23rd ESV Conference, Seoul, Korea, May, 2013.

10. Quaglia, G., Sorli, M. “Air Suspension Dimensionless Analysis and Design Procedure,” Vehicle System Dynamics, Vol. 35, No. 6, 2001, pp. 443-475.

11. Nakajima, T., Shimokawa, Y., Mizuno, M., Sugiyama, H., “Air Suspension System Model Coupled with Leveling and Differential Pressure Valves for Railroad Vehicle Dynamics Simulation,” Journal of Computational and Nonlinear Dynamics, Vol.9, 2014, July, 2014, pp 031006 1-9. doi: 10.1115/1.4026175.

12. Hao, L., Jaecheon, L., “Model Development of Automotive Air Spring Based on Experimental Research,” Third International Conference on Measuring Technology and Mechatronics Automation, 2011. DOI 10.1109/ICMTMA.2011.433

13. Sadeghi Reineh, M. and Pelosi, M., “Physical Modeling and Simulation Analysis of an Advanced Automotive Racing Shock Absorber using the 1D Simulation Tool AMESim,” SAE International Journal of Passenger Cars, Vol.6, No. 1, 2013, pp.7-17, doi:10.4271/2013-01-0168.

14. Edmond, R., Yildirim, H,. “A High Performance Pneumatic Force Actuator System Part 1- Nonlinear Mathematical Model,” ASME Journal of Dynamic System Measurement and Control, Vol. 122, No.3, 2000, pp. 416-425

Nomenclature and General Data

p_s Airspring absolute pressure (psi)

T_s Airspring temperature (K)

V_s Airspring volume (in^3)

R Gas constant ($ft \cdot lb/slug \cdot {}^0R$)

M_s Molar mass (slugs/mol)

P_{s0} Airspring initial pressure (psi)

T_{s0} Airspring initial temperature (K)

V_{s0} Airspring initial volume (in^3)

n Polytropic exponent

h Height of airspring (in)

A Effective area of airspring (in^2)

F Force exerted by airspring (lbf)

p_a Atmosphere pressure (psi)

p_u Upstream pressure (psi)

p_d Downstream pressure (psi)

S Effective area of leveling valve (in^2)

b Critical pressure

T_l Leveling valve temperature (K)

T Tube temperature (K)

P End pressure in the tube (psi)

c Sound velocity (in/s)

L_t Tube length (in)

u Flow velocity in the pipe (in/s)

D Inner diameter in the tube (in)

f Friction factor

μ Dynamic viscosity of air ($lbf \cdot s/in^2$)

k_{sij} Spring stiffness (lbf/in)

k_{uij} Wheel stiffness (lbf/in)

C_{sij} Damping constant ($lbf \cdot s/in$)

F_{Cij} Damping force (lbf)

F_{Kij} Leaf spring/ Airspring force (lbf)

The middle subindex i=f, m, r

f *Front axle*

m *Middle axle*

r *Rear axle*

The rear subindex j=l, r

l *Left*

r *Right*

m Vehicle body mass (slugs)

a Distance from CG to front axle (in)

b_1 Distance from CG to middle axle (in)

b_2 Distance from CG to rear axle (in)

c Front wheel track (in)

d Rear wheel track (in)

F_0 Initial load force (lbf)

Abbreviations

OE Original Equipment

CG Center of Gravity

Appendix A

Table 1. Main parameters selected for pneumatic suspension simulation

Parameter	Value(English unit)	Value(SI unit)
Airspring initial pressure, p_t	70 psi	482633 pa
Initial effective area of airspring, A_0	75 in^2	0.1936 m^2
Airspring initial height, h_0	10 in	0.254 m
Air tank pressure, p_{ta}	120 psi	827370.88 pa
Atmospheric pressure, p_a	14.7 psi	101300 pa
Initial temperature T_0	68 F^0	293.15 K
Dead band of leveling valve(Balanced)	$\pm$0.16 in	$\pm$0.004 m
Dead band of leveling valve(OE)	$\pm$0.32 in	$\pm$0.008 m
Pipe inner diameter(Balanced)	0.4 in	0.01016 m
Pipe inner diameter(OE)	0.236 in	0.006 m
Pipe absolute roughness rr	4.7244 e-6 in	0.00012 mm

Appendix B

Table 2. Main parameters selected for truck multibody dynamic simulation

Parameter	Value(English unit)	Value(SI unit)
Body (sprung) weight(loaded)	28357.824 lbf	126141.885 N
Roll moment of inertia, I_r	158044.1 $lbf \cdot in \cdot s^2$	17855.7 $kg \cdot m^2$
Pitch moment of inertia, I_p	632176.5 $lbf \cdot in \cdot s^2$	71422.8 $kg \cdot m^2$
Front leaf spring stiffness per suspension	692.71 lbf/in	121306 N/m
Front damping constant per suspension	97.36 $lbf \cdot s/in$	17049.3 $N \cdot s/m$
Rear damping constant per suspension	164.72 $lbf \cdot s/in$	28845.6 $N \cdot s/m$
Front unsprung weight per suspension	700 lbf	3114.97 N
Rear unsprung weight per suspension	1000 lbf	4450 N
Front unsprung stiffness per suspension	5250 lbf/in	919370 N/m
Rear unsprung stiffness per suspension	10500 lbf/in	1838740 N/m
Distance from the CG to the front axle, a	163 in	4.1402 m
Distance from the CG to the middle axle, b_1	30 in	0.762 m
Distance from the CG to the rear axle, b_2	84 in	2.1336 m
Front wheel track, c	80 in	2.032 m
Rear wheel track, d	76 in	1.9304 m

Appendix C

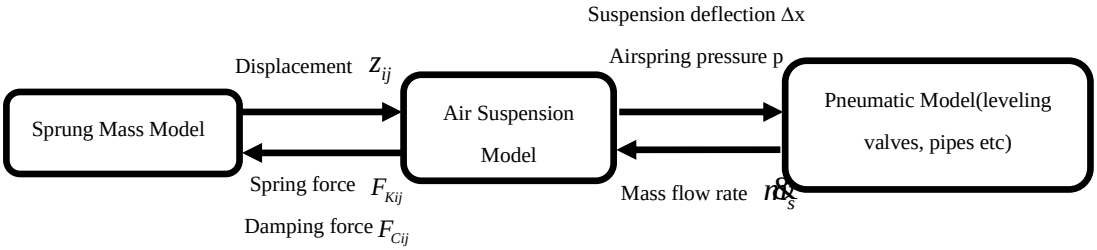

Figure 20. Relationship between truck dynamic model and pneumatic system model

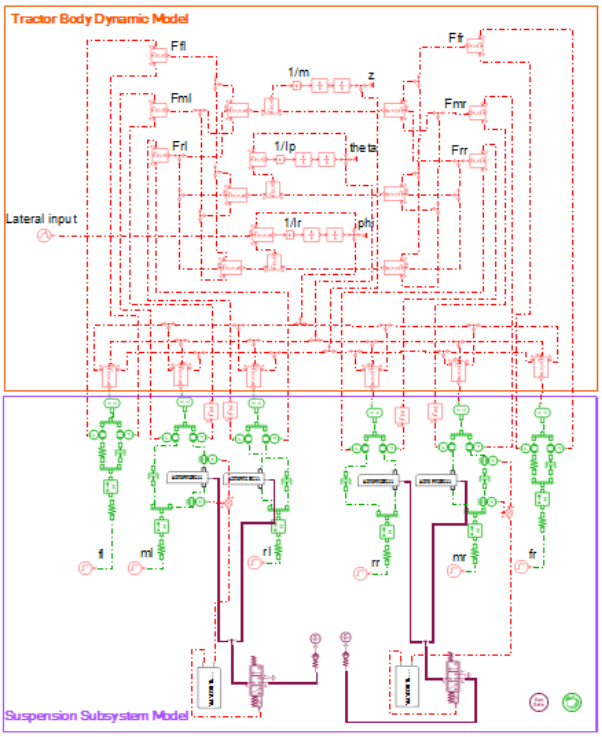

Figure 21. Aligned system model with balanced pneumatic suspension in AMEsim